Epitope Mapping of the Phosphorylation Motif of the HIV-1 Protein Vpu Bound to the Selective Monoclonal Antibody Using TRNOESY and STD NMR Spectroscopy†

Josyane Gharbi-Benarous,‡ Gildas Bertho,‡ Nathalie Evrard-Todeschi,‡ Gaël Coadou,‡ Simon Megy,‡ Thierry Delaunay,§ Richard Benarous,|| and Jean-Pierre Girault*,‡

Laboratoire de Chimie et Biochimie Pharmacologiques et Toxicologiques (UMR 8601 CNRS), Université René Descartes-Paris V, 45 rue des Saint-Pères, 75270 Paris Cedex 06, France, U567-INSERM, UMR 8104 CNRS, Institut Cochin-Département des Maladies Infectieuses, Hôpital Cochin Bat. G. Roussy, 27 rue du Faubourg St-Jacques, 75014 Paris, France, and UMR GDPP, INRA-Université Bordeaux 2, 71 Avenue Edouard Bourleaux, 33883 Villenave D'Ornon Cedex, France

Received April 9, 2004; Revised Manuscript Received September 14, 2004

ABSTRACT: The conformational preferences of a 22-amino acid peptide (LIDRLIERAED**pS**GNE**pS**EGEISA) that mimics the phosphorylated HIV-1-encoded virus protein U (Vpu) antigen have been investigated by NMR spectroscopy. Degradation of HIV receptor CD4 by the proteasome, mediated by the HIV-1 protein Vpu, is crucial for the release of fully infectious virions. Phosphorylation of Vpu at sites Ser52 and Ser56 on the DSGXXS motif is required for the interaction of Vpu with the ubiquitin ligase SCF$^{\beta-\mathrm{TrCP}}$ which triggers CD4 degradation by the proteasome. This motif is conserved in several signaling proteins known to be degraded by the proteasome. The interaction of the P-Vpu$^{41-62}$ peptide with its monoclonal antibody has been studied by transferred nuclear Overhauser effect NMR spectroscopy (TRNOESY) and saturation transfer difference NMR (STD NMR) spectroscopy. The peptide was found to adopt a bend conformation upon binding to the antibody; the peptide residues (Asp51−pSer56) forming this bend are recognized by the antibody as demonstrated by STD NMR experiments. The three-dimensional structure of P-Vpu$^{41-62}$ in the bound conformation was determined by TRNOESY spectra; the peptide adopts a compact structure in the presence of mAb with formation of several bends around Leu45 and Ile46 and around Ile60 and Ser61, with a tight bend created by the D**pS**^{52}GNE**pS**^{56} motif. STD NMR studies provide evidence for the existence of a conformational epitope containing tandem repeats of phosphoserine motifs. The peptide's epitope is predominantly located in the large bend and in the N-terminal segment, implicating bidentale association. These findings are in excellent agreement with a recently published NMR structure required for the interaction of Vpu with the SCF$^{\beta-\mathrm{TrCP}}$ protein.

Vpu is unique to HIV-1,[1] the major causative agent of acquired immune deficiency syndrome, and is not found in other lentiviruses such as HIV-2 (which is less pathogenic than HIV-1) or in most simian immunodeficiency viruses (SIVs). Vpu is an integral membrane protein of 81 amino acids (Figure 1a). It was shown (Figure 1b) that its secondary structure consists of one transmembrane hydrophobic helix (h1) near the N-terminus and two amphipathic helices (h2 in-plane and h3) in the cytoplasmic C-terminal domain, using a combination of solid-state NMR and solution NMR methods (*1*). The protein has two principal biological functions that contribute to the virulence of HIV-1 infections in humans, and which are associated with different structural domains of the protein. Vpu enhances the release of new virus particles from the plasma membrane of cells infected with HIV-1 (*2*) through its N-terminal transmembrane domain (h1), whereas it induces the degradation of the CD4 receptor in the endoplasmic reticulum (*3*, *4*) via its cytoplasmic domain (h2 and h3). It has been demonstrated that Vpu binds to the F-box WD40 protein β-transducin repeat-containing protein (β-TrCP), the receptor component of the multisubunit SCF$^{\beta-\mathrm{TrCP}}$ E3 ubiquitin ligase complex, and connects CD4 to the ubiquitin−proteasome machinery to promote CD4 degradation and produce fully infectious particles (*5*). β-TrCP interacts with Vpu through its C-terminal WD repeat region (*5*). Evidence that the Vpu−β-TrCP interaction depends on the phosphorylation of the

† This work was supported by grants from Sidaction, ANRS (Agence Nationale pour la recherche contre le SIDA), and ARC (Association pour la Recherche sur le Cancer).

* To whom correspondence should be addressed. Telephone: 33 (0)1 42 86 21 80. Fax: 33 (0)1 42 86 83 87. E-mail: Jean-Pierre.Girault@univ-paris5.fr.

‡ Université René Descartes-Paris V.

§ INRA-Université Bordeaux 2.

|| Institut Cochin-Département des Maladies Infectieuses.

[1] Abbreviations: ARIA, ambiguous restraints for iterative assignment; mAb, monoclonal antibody; β-TrCP, β-transducin repeat-containing protein; SCF, Skp1-Cullin-FBox; HIV, human immunodeficiency virus; HSQC, heteronuclear single-quantum correlation; MD, molecular dynamics; NOESY, nuclear Overhauser effect spectroscopy; Vpu, HIV-1 encoded virus protein U; PBS, phosphate-buffered saline; rmsd, root-mean-square deviation; ROESY, rotating frame Overhauser effect spectroscopy; STD, saturation transfer difference; TRNOESY, transferred nuclear Overhauser effect spectroscopy; TRROESY, transferred rotating frame Overhauser effect spectroscopy; TOCSY, total correlation spectroscopy; TPPI, time-proportional phase incrementation; WATERGATE, water suppression by gradient-tailored excitation.

10.1021/bi0492861 CCC: $27.50
Published on Web 10/30/2004

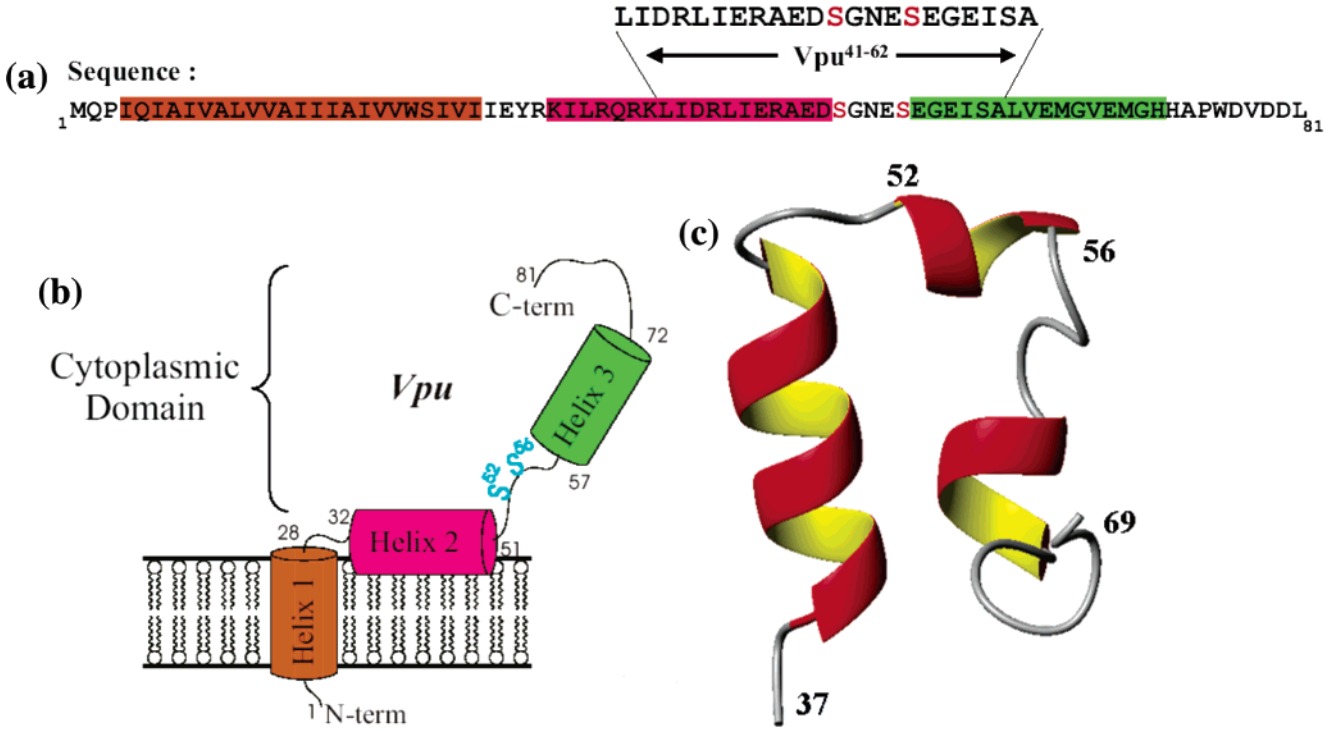

FIGURE 1: (a) Primary structure sequence of the HIV-1 Vpu protein and (top) sequence of the Vpu fragment which was investigated in this work. (b) Domains of the secondary structural regions found in Vpu. The hydrophobic N-terminal membrane anchor (helix h1, residues 1−28) is followed by two amphipathic α-helices (helix h2, residues 32−51; helix h3, residues 57−72). Both helices are joined by a flexible nonstructured link, which contains phosphoacceptors Ser52 and Ser56. The C-terminus forms a reverse turn at Ala74 (*49*). (c) Part of the backbone (residues 37−69) of the Vpu cytoplasmic domain (residues 37−81) structure (*48*).

serine residues at positions 52 and 56 of the Vpu cytoplasmic domain by casein kinase II has been provided (*6*). *β*-TrCP is also involved in the ubiquitination and proteasome targeting of *β*-catenin, the accumulation of which has been implicated in various human cancers (*7*, *8*), I*κ*Bα, the inhibitor of master transcription factor NF*κ*B (*8*−*10*), and ATF4, a member of the family of transcription factors (*11*). The signal for the recognition of all these cellular ligands by *β*-TrCP is the phosphorylation of the serine residues present in a conserved motif, D**pS**GXX**pS** for Vpu, *β*-catenin, and I*κ*Bα and D**pS**GXXX**pS** for ATF4. Antibodies which recognize epitopes implicated in degradation of HIV receptor CD4 by the proteasome have been developed. The antigenic peptides containing the D**pS**GXX**pS** motif constitute *β*-TrCP-associated epitopes. The $SCF^{\beta-TrCP}$ complex specifically recognizes a Vpu peptide fragment of 22 amino acids, a 19-amino acid motif in I*κ*Bα, and a 22-residue *β*-catenin polypeptide in a phosphorylation-dependent manner (*8*). A specific monoclonal antibody (mAb DE7) was generated against the P-Vpu^{41-62} peptide (Figure 1), LIDRLIERAED**pS**GNE**pS**EGEISA (numbers refer to the Vpu protein). We postulate that structural similarities can occur between the small peptide ligand and the same sequence found within the intact protein, so when antiligand monoclonal antibodies recognizing the peptide were obtained, they are very good tools for the evaluation of structural elements of the intact protein bound by the natural receptor (*β*-TrCP). This antibody is specific to the native phosphorylated Vpu containing the DpS^{52}GNEpS^{56} amino acid sequence in the central part, and does not react with the nonphosphorylated protein. In addition, we showed previously that the P-Vpu^{41-62} phosphorylated peptide has structural features different from those of its parent Vpu^{41-62} peptide (*12*).

Antibody DE7 recognizes the P-Vpu^{41-62} peptide, a small antigen-binding fragment, and a fragment generally retains the specificity and affinity of the entire parent protein. Antireceptor antibodies have been successfully used for the investigation of ligand−receptor interactions as the internal complementary binding region of the receptor binding site (*13*, *14*). This latter approach can be especially useful when (a) isolation of the receptor in a suitable form for structural studies of the receptor−ligand interaction is extremely difficult or (b) little information is available for its active state (*15*). Thus, determination of the conformational features of the Vpu D**pS**GXX**pS** moiety implicated in antibody binding should provide complementary information about the structural parameters characterizing Vpu−*β*-TrCP receptor interaction (*16*) to improve the understanding of the substrate specificity of $SCF^{\beta-TrCP}$. The structural characterization of the D**pS**GXX**pS** moiety may have an additional interest. This will contribute to the design of molecules mimicking the structure of the Vpu adhesion site and possibly thus acting as a potent model for the D**pS**GXX**pS**−protein complex.

Here, we present the STD NMR epitope mapping and TRNOE-based conformational analysis of the P-Vpu^{41-62} peptide bound to the monoclonal antibody, mAb DE7. The TRNOESY experiment has been used to determine the conformations of a wide range of small ligands in the protein-bound state by focusing on the easily detected NMR signals of the free ligands (*17*). The mAb-bound P-Vpu^{41-62} peptide conformation was finally elucidated by molecular dynamics simulation, an approach combining dynamical annealing and refinement protocols. Saturation transfer difference (STD) NMR (*18*−*20*) is a technique that can be used to characterize

and identify binding. It can also be used to identify the binding epitope of ligands to a protein receptor (*20*). These techniques, used to probe the conformation of a ligand bound to a protein receptor, have become increasingly important as a tool in the investigation of biomolecular recognition phenomena (*21*, *22*), as well as for the binding of antigenic peptides to mAbs (*23*−*25*).

MATERIALS AND METHODS

Peptides. HIV-1-encoded virus protein U (Vpu) fragments (residues 41−62), the P-Vpu$^{41-62}$ peptide containing phosphorylated sites 52 and 56, with the LIDRLIERAED**pS**GNE**pS**EGEISA amino acid sequence, were purchased from Neosystem Lab. (Strasbourg, France). The purity of the peptides (95%) was tested by analytical HPLC and by mass spectrometry.

Monoclonal Antipeptide Antibody. Monoclonal anti-diphospho-Vpu (pSer^{52} and pSer^{56}) (mouse IgG1 isotype) is derived from BALB/c mouse immunized with a synthetic peptide corresponding to amino acids 41−62 (pSer^{52} and pSer^{56}) of Vpu coupled to BSA as a protein carrier. Following the fusion and the first two weeks of culture, the hybridoma culture supernatants were screened with an ELISA for the presence of antibody. Three ELISA formats were developed: (1) direct binding of the peptide coated to the ELISA plate, (2) direct binding of the biotinylated peptide linked to the streptavidin absorbed on the ELISA plate and, and (3) binding of the free biotinylated peptide in liquid phase by the monoclonal antibodies absorbed on the ELISA plate and revelation by the peroxidase−streptavidin complex. Non-phosphorylated peptides, biotinylated or not, were used as a negative control.

The selected antibody was determined to be of the IgG1 isotype and was purified from bulk culture supernatant on a protein G affinity column. The sample was then dialyzed in standard PBS buffer and filtered through a 0.22 μm membrane. The antibody concentration was determined by optical density measurement at 280 nm using an absorption coefficient of 1.35. Its concentration was estimated to be ~0.71 mg/mL in a volume of 12.5 mL. Thus, the quantity of purified antibody was ~8.9 mg with an approximate molecular mass of 150 kDa. This amount of purified antibody was used to prepare the NMR samples.

NMR Experiments. ^{1}H NMR spectra were recorded at 280 K on a Bruker AMX-500 spectrometer using a *z*-axis gradient. Chemical shift assignments (Tables 1 and 2) refer to internal 3-(trimethylsilyl)propionic acid-2,2,3,3-d_4, sodium salt (TSP-d_4). Two-dimensional NMR spectra were recorded in the phase-sensitive mode using the States−TPPI method (*26*). All experiments were carried out using the WATERGATE pulse sequence for water suppression (*27*). Two-dimensional ^{1}H−^{1}H TOCSY spectra were recorded using a MLEV-17 spin-lock sequence (*28*) with a mixing time of 70 ms. Typically, spectra were acquired with 256 t_1 increments, 2048 data points, and a relaxation delay of 1.5 s. Spectra were processed using XWINNMR software. All spectra were zero-filled in the F_1 spectral dimension to 1024 data points, and a sine bell window function was applied in both dimensions prior to Fourier transformation. For preparation of NMR peptide−antibody samples, the antibody solution was diluted several times in NMR phosphate-buffered saline (20 mM phosphate, 5% D_2O, and 0.02% NaN_3) at pH 7.2 and concentrated using Amicon Ultra-15 centrifugal filters from Millipore with a 30 kDa molecular mass cutoff.

For STD experiments (Figure 2), the ligand:antibody ratio was increased to 20:1 (2 mM P-Vpu$^{41-62}$ peptide, 100 μM mAb DE7). The one-dimensional (1D) ^{1}H STD NMR (*18*−*20*) spectra of the mAb DE7−peptide complex (Figure 2) were recorded at 500 MHz with 2048 scans and selective

Table 1: ^{1}H NMR Chemical Shifts (parts per million) of the Free P-Vpu$^{41-62}$ Peptide from TSP-d_4[a]

residue	δNH	δH$_\alpha$	δH$_\beta$	δH$_\gamma$	δH$_\delta$	δ others
Leu41	−	4.06	1.73, 1.67	1.67	0.97	
Ile42	−	4.22	1.85	1.52, 1.22	0.89	
Asp43	8.60	4.59	2.74, 2.59			
Arg44	8.43	4.32	1.88, 1.78	1.64	3.22	7.37, 7.02, 6.65
Leu45	8.53	4.34	1.73, 1.63	1.61	0.96, 0.89	
Ile46	8.05	4.17	1.88	1.50, 1.21	0.91, 0.88	
Glu47	8.58	4.28	2.04, 1.94	2.28, 2.24		
Arg48	8.45	4.38	1.89, 1.79	1.66	3.22	7.45, 7.02, 6.65
Ala49	8.71	4.32	1.45			
Glu50	8.60	4.28	2.10, 1.96	2.31		
Asp51	8.39	4.67	2.78, 2.70			
pSer52	8.91	4.52	4.12			
Gly53	8.74	4.00				
Asn54	8.38	4.80	2.87, 2.76	7.87, 7.05		
Glu55	8.73	4.34	2.11, 1.98	2.32		
pSer56	8.87	4.55	4.11, 4.06			
Glu57	8.78	4.30	2.13, 2.00	2.34		
Gly58	8.44	4.03, 3.93				
Glu59	8.41	4.32	2.03, 1.95	2.30, 2.24		
Ile60	8.48	4.23	1.89	1.53, 1.23	0.94	
Ser61	8.61	4.49	3.87			
Ala62	8.22	4.16	1.37			

[a] Spectra were recorded at 280 K and pH 7.2 in 20 mM sodium phosphate and a 9:1 H_2O/^2H_2O mixture (by volume). Resonances of protons marked with a dash were not visible.

Table 2: ^{1}H NMR Chemical Shifts (parts per million) of the P-Vpu$^{41-62}$ Peptide Bound to Antibody mAb DE7 from TSP-d_4[a]

residue	δNH	δH$_\alpha$	δH$_\beta$	δH$_\gamma$	δH$_\delta$	δ others
Leu41	−	4.07	1.73	1.66	0.96	
Ile42	8.50	4.23	1.87	1.52; 1.22	0.93	
Asp43	8.61	4.59	2.73, 2.58			
Arg44	8.45	4.31	1.87, 1.78	1.63	3.22	7.34, 7.00, 6.65
Leu45	8.53	4.33	1.72	1.59	0.94, 0.88	
Ile46	8.08	4.16	1.88	1.47, 1.19	0.91	
Glu47	8.58	4.28	2.07, 1.95	2.24		
Arg48	8.47	4.36	1.88, 1.79	1.65	3.22	7.42, 7.00, 6.65
Ala49	8.71	4.32	1.43			
Glu50	8.61	4.28	2.07, 1.95	2.32		
Asp51	8.41	4.67	2.77, 2.70			
pSer52	8.89	4.53	4.13			
Gly53	8.73	4.00				
Asn54	8.37	4.80	2.86, 2.75	7.86, 7.05		
Glu55	8.73	4.33	2.15, 1.99	2.31		
pSer56	8.86	4.55	4.12, 4.07			
Glu57	8.77	4.30	2.20, 2.01	2.32		
Gly58	8.43	4.02, 3.94				
Glu59	8.42	4.32	2.02, 1.95	2.30, 2.24		
Ile60	8.50	4.23	1.87	1.52, 1.22	0.93	
Ser61	8.63	4.49	3.87			
Ala62	8.24	4.16	1.36			

[a] Spectra were recorded at 280 K at pH 7.2 with a 10:1 P-Vpu:mAb DE7 ratio, and 20 mM sodium phosphate in a 9:1 H_2O:^2H_2O mixture (by volume). Resonances of protons marked with a dash were not visible.

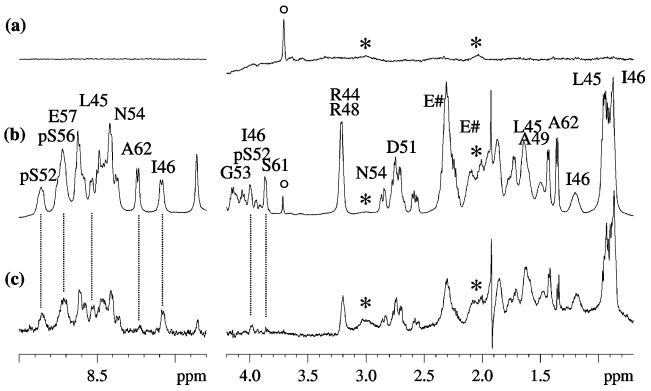

FIGURE 2: Epitope mapping of the P-Vpu$^{41-62}$ peptide in the presence of mAb DE7, for a peptide:antibody ratio of 20:1. (a) Reference 1D NMR spectrum of the 150 kDa antibody mAb DE7 displaying few broad signals (asterisk) at 3.00 and 2.05 ppm, normal for an antibody and a sharp resonance signal (degree) at 3.72 ppm arising from low-molecular mass impurity. (b) Reference 1D ^{1}H spectrum of the P-Vpu$^{41-62}$ peptide in association with the mAb DE7 antibody. (c) 1D ^{1}H STD NMR spectrum of the P-Vpu$^{41-62}$ peptide in association with the mAb DE7 antibody, showing enhancements of resonances of protons making close contacts with the antibody-combining site; one can see that the impurity contained in spectrum a is effectively subtracted and therefore does not give rise to a signal in the difference STD spectrum.

saturation of protein resonances at 12 or −3 ppm (30 ppm for reference spectra) showing that by irradiating at −3 ppm, the entire protein can be saturated uniformly and can therefore be efficiently used for the STD NMR technique. Investigation of the time dependence of the saturation transfer with saturation times from 0.2 to 4.0 s showed that 2 s was needed for efficient transfer of saturation from the protein to the ligand protons. STD NMR spectra were acquired using a series of 40 equally spaced 50 ms Gaussian-shaped pulses for selective saturation (then, a total saturation time was approximately 2.0 s) (*29*), with a 1 ms delay between the pulses. With an attenuation of 50 dB, the radio frequency field strength for the selective saturation pulses in all STD NMR experiments was 190 Hz. Subtraction of FID values with on- and off-resonance protein saturation was achieved by phase cycling.

Transferred nuclear Overhauser effect (TRNOESY) (*30*) spectra of the mAb DE7−peptide complex were recorded with 4K points and 512 t_1 increments, and a relaxation delay of 1.5 s (Figure S7a in the Supporting Information). Data processing was performed by zero filling to 1K points in F_1 to give a final 4K × 1K matrix followed by multiplication with a squared cosine function and Fourier transformation. The bound and free states exist in the same regime, namely, $\omega\tau_c > 1$; thus, the cross-relaxation rates of the P-Vpu$^{41-62}$ peptide (MW = 2563 g/mol) in the free and bound state are negative in sign. The optimal conditions for the TRNOESY measurements were determined by considering a peptide:mAb molar ratio ranging from 10 to 100 with mixing times (τ_m) of 50, 100, 200, 300, and 500 ms. After optimization of the P-Vpu$^{41-62}$ peptide:antibody ratio, the final NMR sample was prepared with 7.5 mg of mAb DE7 (0.1 mM antibody) and 1.3 mg of P-Vpu$^{41-62}$ (1.0 mM), which corresponds to a peptide:antibody ratio of 10:1, in 500 μL of buffer solution at pH 7.2. The buildup curve (*31*) for different NOE correlations showed that spin diffusion was negligible for a τ_m of 200 ms (Figure S8 in the Supporting Information). The observed TRNOE correlations with mixing times of 100 and 200 ms were large and negative. They were assigned to the mAb-bound antigen (*23*) as a sample of the peptide without the presence of antibody exhibited only intraresidue and sequential NOE intensities with a mixing time of 200 ms (Figure S7b in the Supporting Information). Automatic baseline correction was performed prior to integration of cross-peak volumes using FELIX (Biosym Technologies). Cross-peak intensities were converted to interproton distances using the distance between the Asn NH_2 protons (1.73 Å) as a reference. TRNOE cross-peaks classified as strong, medium, and weak were converted into distance restraints of 1.8−2.7, 1.8−3.6, and 1.8−6.0 Å, respectively. With regard to the spin diffusion effect, we conducted a TRROESY experiment to check the validity of the observed TRNOEs. Therefore, for direct comparison with TRNOESY (τ_m = 200 ms), TRROESY with the mixing time of 100 ms must be used (Figure S9 in the Supporting Information). Interresidue ^{1}H−^{1}H distances (Table S5 in the Supporting Information) deduced from ROE and NOE volumes are in agreement. The two-dimensional ROESY spectra were recorded with a mixing time of 100 ms and 64 scans for each of the 512 t_1 increments using a spin lock field of 1190 Hz (γB_1) at 5.0 ppm. It is usually assumed that TRROESY can be interpreted on the assumption that, at least for short mixing times, spin diffusion effects can be ignored. Nevertheless, the use of TRROESY to test spin diffusion can be limited, and when possible, a good approach to exploiting nuclear Overhauser effects to determine internuclear distances between pairs of protons, without perturbation of spin diffusion effects, should be the QUIET-TRNOESY NMR experiment (*32*, *33*). The conventional NOESY experiment is modified by inserting a doubly selective radio frequency pulse in the middle of the mixing time to invert two spectral regions selected to include the chemical shifts of a "source" and a "target" proton (*34*).

Structure Calculations. Distance restraints used in the structure calculations were derived from TRNOESY experiments performed with mixing times of 100 and 200 ms, and as for the free ligand, we obtained a blank TRNOESY spectrum at 100 ms and only intraresidue and sequential NH−Hα correlations at 200 ms. The final list of distant restraints containing 193 unambiguous (89 intraresidue, 50 sequential, 25 medium-range, and 29 long-range) and 44 ambiguous (15 intraresidue, 9 sequential, 6 medium-range, and 15 long-range) restraints (Table 3) was incorporated for structure calculation with the standard protocol of ARIA 1.2 (*35*, *36*). Modifications of the phosphorylated residues (pSer) were introduced with CHARMM (*37*) for molecular dynamics calculations using the PARALLHDG 5.3 force field. During the calculations, non-glycine residues were restrained to negative ϕ values (usually the only range considered in NMR-derived structures) (*38*). The simulated annealing protocol consisted of four stages: a high-temperature torsion angle simulated annealing phase at 10 000 K (1100 steps), a first torsion angle dynamics cooling phase from 10 000 to 2000 K (550 steps), a second Cartesian dynamics cooling phase from 2000 to 1000 K (5000 steps), and a third Cartesian dynamics cooling phase from 1000 to 0 K (2000 steps). ARIA enabled the incorporation of ambiguous distance restraints and calibration of the NOE restraints using automated matrix analysis as implemented by the program.

Table 3: Structural Statistics of the Final 10 NMR Structures of P-Vpu$^{41-62}$ Bound to the mAb DE7 Antibody

	$ARIA_{output}$
no. of experimental distance restraints	
unambiguous NOE	193[a]
ambiguous NOE	44[b]
total NOEs	237
no. of experimental broad dihedral restraints	18
rms differences from distance restraints[c]	
unambiguous NOE (Å)	0.1 ± 0.09
ambiguous NOE (Å)	0.08 ± 0.06
all NOEs (Å)	0.1 ± 0.08
NOE violations >0.5 Å	1
NOE violations >0.3 Å	2
rms differences from mean structure[d] (Å)	
backbone	1.79 ± 0.73
heavy	3.05 ± 0.83
Ramachandran plot of residues[e]	
in most favored regions	28 (56)
in additional allowed regions	61 (39)
in generously allowed regions	11 (5)
in disallowed regions	0 (0)

[a] NOEs: 89 intraresidue, 52 sequential, 23 medium-range, and 29 long-range. [b] NOEs: 15 intraresidue, 9 sequential, 6 medium-range, and 14 long-range. [c] Calculated with ARIA. [d] Calculated with MOLMOL. [e] Calculated with PROCHECK, and between parentheses are the values for the bound structure with the lowest energy.

ARIA runs were performed using the default parameters with eight iterations. Twenty structures were generated each round, and the 10 lowest-energy structures were carried on to the next iteration. In the final iteration, the 20 lowest-energy structures were retained as the final structures. The set of P-Vpu$^{41-62}$ structures was selected for correct geometry and no distance restraint violations of >0.5 Å. Analysis of the structures was performed within AQUA, PROCHECK-NMR (*30*) programs (Table 3). MOLMOL (*39*) was used for the analysis and presentation of the results of the structure determination (Table S4 in the Supporting Information).

RESULTS

Binding of mAb to the Phosphorylated P-Vpu$^{41-62}$ Peptide. The monoclonal anti-diphospho-Vpu (pSer52 and pSer56) reacts specifically with the Vpu diphosphorylated at Ser52 and Ser56. At the peptide level, the antibody recognizes efficiently the P-Vpu$^{41-62}$ peptide but not the nonphosphorylated one. The mAbs were tested in a direct ELISA for binding to block the P-Vpu$^{41-62}$ peptide, which contained the consensus DpSGXXpS sequence. The P-Vpu$^{41-62}$ peptide inhibited mAb binding with an IC_{50} of ~2 mM. Given the uncertainties in the effective concentration of mAb that was immobilized on the ELISA plate, the K_D for the P-Vpu$^{41-62}$ peptide bound to mAb was estimated to be between 100 and 500 μM. This range of binding affinity made the peptide likely to be suitable for TRNOESY NMR experiments, which require fast exchange between the free and bound states.

NMR Resonance Assignments. ^{1}H chemical shifts and Resonance assignments were established using two-dimensional ^{1}H−^{1}H TOCSY and NOESY experiments (*40*) and are reported in Tables 1 and 2. Sequential assignments of ^{1}H resonances were based on characteristic sequential NOE connectivities observed between the α-proton of residue *i* and the amide proton of residue *i* + 1, i.e., $d_{\alpha N}(i, i+1)$ in the NOESY data set. Interestingly, in the presence of antibody, a slight downfield shift of the amide protons was observed in the terminal regions, residues 43−48 in the N-terminal region and residues 59−62 in the C-terminal region; however, observation of an opposite shift, upfield-shifted HN resonances only for pSer52 at Gly53 and Asn54 and for pSer56 at Glu57 and Gly58 may be an indicator of intermolecular contact of the phosphorylated motif with the binding site (Figure 3).

Interaction of P-Vpu$^{41-62}$ with mAb DE7. In the presence of the antibody, selective line broadening of the resonances of only the phosphorylated peptide was observed, indicating binding of the peptide to the antibody. The dissociation constant was estimated from the line broadening at different peptide:antibody ratios to be ~200 μM (*17*). These measurements show that the phosphorylated D**pS**GNE**pS** motif is necessary for binding, but residues from the longer peptide P-Vpu$^{41-62}$ do contribute additional binding energy. Because of the low mAb DE7:peptide molar ratio, free and bound peptide molecules were in rapid chemical exchange and only a single set of broadened ligand resonances was observed. To provide additional information regarding the peptide mode of binding, STD NMR experiments were performed (*18*−*20*). The STD NMR technique is a method of epitope mapping by NMR spectroscopy. Resonances of the protein are selectively saturated, and in a binding ligand, enhancements are observed in the difference (STD NMR) spectrum resulting from subtraction of this spectrum from a reference spectrum in which the protein is not saturated (*18*−*20*). Protons of the ligand which are in close contact with the protein can easily be identified from the STD NMR spectrum, because they are saturated to the highest degree. They should have stronger STD, and this allows direct observation of areas of the ligand that comprises the epitope. The different signal intensities of the individual protons are best analyzed from the integral values in the reference (I_0) and STD spectra ($I_0 - I_{sat}$). The integral value of the largest signal of the P-Vpu$^{41-62}$ peptide, the pSer52 H−N proton, was set to 100%. The relative degree of saturation for the individual protons, normalized to that of pSer52, can be used to compare the STD effect (*20*).

We investigated the interaction of the P-Vpu$^{41-62}$ peptide with mAb DE7. The STD NMR spectrum of the P-Vpu$^{41-62}$ peptide in the presence of the antibody is shown in Figure 2. For reference, the STD NMR spectrum was recorded with a sample containing the nonphosphorylated Vpu$^{41-62}$ peptide, and all signals from the nonbinding peptide are completely eliminated. Figure 2 shows the 1D STD spectrum and a normal ^{1}H spectrum of the complex of P-Vpu$^{41-62}$ with the antibody. The 1D ^{1}H NMR spectrum of P-Vpu$^{41-62}$ in the presence of the mAb DE7 antibody displayed few broad signals at 3.00 and 2.05 ppm, normal for an antibody, and a sharp resonance signal at 3.72 ppm arising from a low-molecular weight impurity (Figure 2). This latter peak was not present in the corresponding STD spectra because this impurity does not bind to the mAb DE7 antibody. The pSer52 (100%) and pSer56 (90%) H−N resonances, and other **pS**GNE**pS** motif resonances belonging to either Asn54 (65%), Glu55 (60%), or Glu57 (70%), have similar STD intensities between 60 and 100%. Obviously, they become more saturated because of the protein than the remaining residues of the ligand and therefore have more and tighter contacts to the antibody's surface. On the other hand, side chain methyl resonances and H−N resonances of Leu45

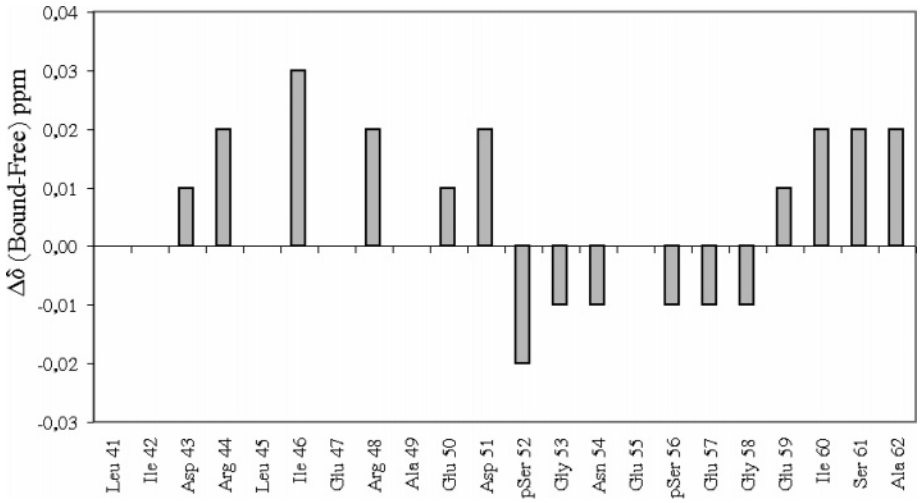

FIGURE 3: Difference for the 22 residues of P-Vpu$^{41-62}$ between the chemical shift of a given resonance free in buffer solution and the chemical shift in the presence of the mAb DE7 antibody plotted versus residue number at 280 K and pH 7.2, for NH resonances.

(90%), Ile46 (85%), and Ala49 (70%) have similar larger STD intensities, ranging from 70 to 90%, indicating that these side chains are involved in the epitope. The lowest intensities correspond to the protons of the C-terminal group, Ile60 (32%), Ser61 (25%), and Ala62 (22%), which reach values of only 20−30%. Thus, a clear distinction between protons with a strong contact to the protein and the others can be made.

The combination of STD NMR epitope mapping data with knowledge of the bound conformation of the ligand, which may be obtained by TRNOESY experiments, is a powerful method for building up models of antibody−ligand interaction (*32*, *41*). Therefore, TRNOESY experiments (*30*, *42*−*44*) were used to investigate the bound conformation of the peptide. A TRNOESY spectrum is shown in Figure S7 in the Supporting Information, whereas the free P-Vpu$^{41-62}$ peptide exhibited only intraresidue and sequential NH−Hα correlations when the mixing times was 200 ms and negative NOE connectivities only for long mixing times ($\tau_m \geq 500$ ms) in aqueous solution and in the absence of mAb DE7 (*12*). A summary of sequential $d(i, i + 1)$ and medium-range $d(i, i + 2)$ and $d(i, i + 3)$ ^{1}H−^{1}H NOE connectivities is presented in Figure 4. We showed that when the peptide: mAb molar ratio was varied from 10 to 100, the optimal conditions for the TRNOESY measurements were observed for a ratio near 10:1. The observation of TRNOE cross-peaks, when mAb DE7 was added, attested to peptide−antibody interaction and the restricted flexibility of the mAb-bound peptide. The NMR signals of the P-Vpu$^{41-62}$ peptide in the presence of mAb DE7 were attributed by the combined use of TOCSY and TRNOESY experiments (Table 2). Multiple TRNOESY connectivities between side chain protons of many residues and the main backbone appeared upon addition of the antibody, suggesting that these side chains are rather frozen in the bound state (Figure 4).

Conformation of the Antibody-Bound Phosphorylated P-Vpu$^{41-62}$ Peptide. The bound conformation of the peptide was investigated by TRNOESY experiments. Since the peptide is in fast exchange on the cross-relaxation time scale of the bound peptide, the observed TRNOESY intensities are sums of the bound and free peptide NOEs. In this study, analysis of TRNOEs was simplified since NOEs, which were present for the free peptide, were smaller than those for the

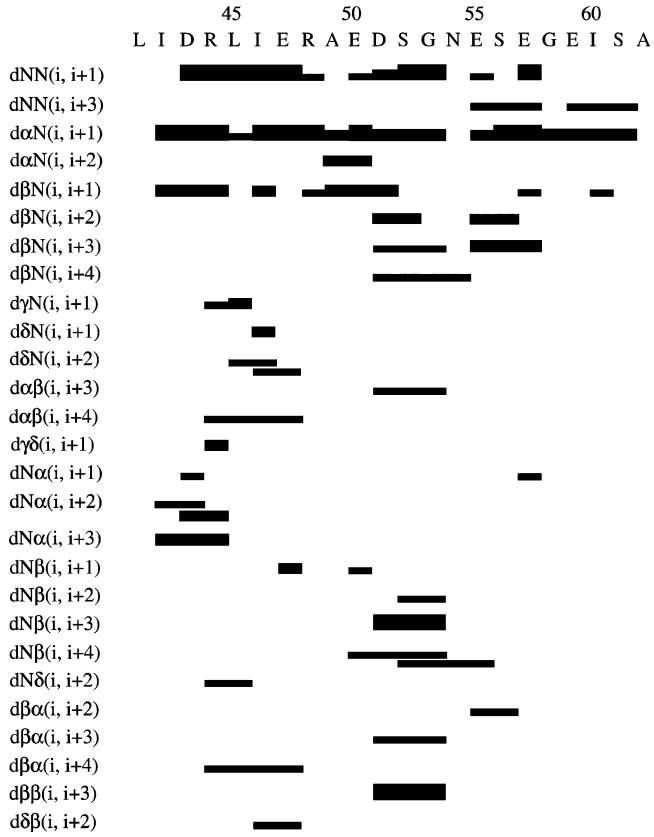

FIGURE 4: Sequential $d(i, i + 1)$ and medium-range $d(i, i + 2)$, $d(i, i + 3)$, and $d(i, i + 4)$ ^{1}H−^{1}H TRNOE connectivities in the P-Vpu$^{41-62}$ peptide (sequence at the top) in the presence of the mAb DE7 antibody at 280 K and pH 7.2. The thickness of the lines reflects the relative intensities of the NOEs within the individual plots.

bound state. With short mixing times (100−200 ms), free peptide NOEs represent small uncorrected NOEs because of the longer mixing times (500−800 ms) used in the free state analysis (Figure S7 in the Supporting Information). For the D**pS**GNE**pS** motif, the TRNOE spectrum exhibits a great number of NOEs, including intense NN(pS52, G53) and NN(G53, N54), medium NN(D51, pS52), and weak NN(E50, D51), NN(E55, S56), and NN(i, $i + 1$) connectivities (Figure 4), suggesting secondary structures (helix, turn, bend, or strand). The presence of consecutive intense αN(i, $i + 1$)

and βN(i, i + 1) NOE connectivities and medium-range αN(i, i + 2), αN(A49, D51), βN(i, i + 2), βN(D51, G53), αβ(i, i + 3), and αβ(D51, N54) NOE connectivities (Figure 4) also denotes the presence of secondary structures. The latter peak argues in favor of a folded structure for the D**pS**GNE**pS** sequence which includes the pSer phosphorylated site. A large number of additional transferred NOE contacts were observed in the presence of the antibody. These included cross-peaks indicative of contacts between the backbone and side chains of the phosphoserine motif pSer52 and Asn54, Asp51 and Asn54, Glu55 and Glu57, and Glu55 and Gly58. The structure was well-defined in the region from Arg48 to Gly58, where a bend was apparent. Strong NN contacts between pSer52 and Gly53 and between Gly53 and Asn54 and other interresidue contacts such as Glu50 Hβ and Asp51 HN and Asp51 Hβ and pSer52 HN helped to define this bend. It is interesting to display the conformational similarity of the binding site at the bend between the bound and free P-Vpu. In the free P-Vpu NOESY spectra with longer mixing times (500−800 ms), the presence of many medium to strong αN(i, i + 1) cross-peaks and no NN(i, i + 3) cross-peaks indicated that residues 50−59 have predominantly β structure. Residues 50−53 are constrained by long-range NOEs, three weak βN(i, i + 2) NOEs [βN(A49, D51), βN(E50, pS52), and βN(D51, G53)], to form a bend in the free P-Vpu$^{41-62}$ peptide. Residues 50−60 have NOE connectivities that suggest the presence of a turn or a half-turn structure: the αN(i, i + 1) and βN(i, i + 1) cross-peaks between residues 53 and 59, one medium NN(i, i + 2) cross-peak [NN(E55, E57)], and two weak γN(i, i + 1) cross-peaks [γN(E55, S56) and γN(E59, I60)]. It is also interesting to show the conformational similarity of the I42−D51 region between bound and free P-Vpu. A large number of transferred NOE contacts were observed in the presence of the antibody. The αN(i, i + 2) [αN(A49−D51)], Nα(i, i + 2) [Nα(I42−R44, D43−L45)], Nδ(i, i + 2) [Nδ(R44−I46)], δN(i, i + 2) [δN(L45−E47), δN(I46−R48)], $\delta\beta$(i, i + 2) [$\delta\beta$(I46, R48)], and Nα(i, i + 3) [Nα(I42−L45)] connectivities are diagnostic of a propensity for a turn region. The pattern of NOE connectivities in the free P-Vpu NOESY spectra suggests that the turns are also present in a water solution in the N-terminal portion of free P-Vpu$^{41-62}$. Turn structure in this segment is implicated by the density of d_{NN} sequential NOEs and the medium-range NOEs such as αN(i, i + 3), αN(D43, I46) and αN(I46, A49). In the free peptide, side chain−side chain NOEs between the βCH_2 protons of Asp43 and βCH_2 and δNH_2 protons of Arg44 and between the βCH_2 and γCH_2 protons of Glu47 and βCH_2 and δNH_2 protons of Arg48 have been observed which suggests the presence of side chain−side chain hydrogen bonding between the NH_2 group of Arg44 and the ϵ oxygen atoms of Glu47 (*12*).

To study the conformation of the bound state of P-Vpu in the presence of the mAb DE7 antibody, the distance restraints were incorporated into a simulated annealing protocol using ARIA. The structures that were generated resulted in NOE restraint files consisting of 193 unambiguous (89 intraresidue, 50 sequential, 25 medium-range, and 29 long-range) and 44 ambiguous (15 intraresidue, 9 sequential, 6 medium-range, and 15 long-range) restraints (Table 3). To differentiate between the probable contribution for each of the ambiguous NOEs, the automated assignment program ARIA was used.

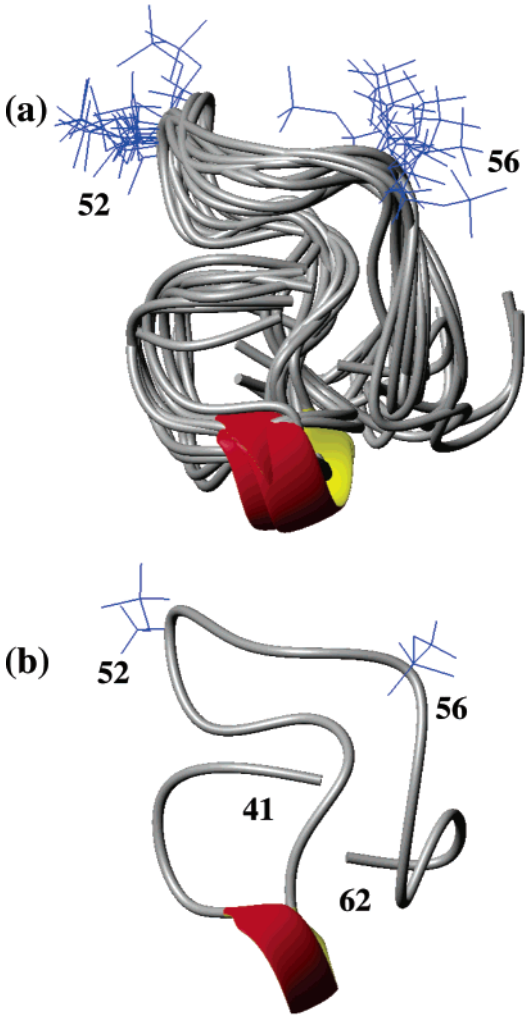

FIGURE 5: NMR TRNOE-derived structures of the bound P-Vpu$^{41-62}$ peptide in the presence of the mAb DE7 antibody. (a) Twenty structures were generated after eight iterations with ARIA software. (b) Minimum energy-minimized conformer with the best fit of proton distance constraints.

Various runs were performed to utilize as many unambiguous and ambiguous restraints as possible from the 500 MHz H_2O TRNOESY spectra. While ARIA has allowed the final structures of the free peptide to undergo a final energy minimization step in a simulated water box, it was decided that due to the presence of the bound peptide in the hydrophobic antibody recognition sites this step was not applicable. A set of 20 structures produced by simulated annealing was subjected to energy minimization, followed by checks for correct geometry and agreement with the distance restraints (Figure 5). The structural models fit the NMR data well, with no violations of experimental distance restraints greater than 0.3−0.5 Å. The positions of the backbone (Table S4 in the Supporting Information) and most side chain atoms were well defined by the NMR restraints. Structural statistics are presented in Table 3. Structure calculations by simulated annealing using NOE constraints followed with refinement and energy minimization led to the family of 10 structures shown in Figure 5a. The calculated structures (Figure 5 and Table 3) comprise a bend from Asp51 to Glu57. This structure would expose the pSer side chains for interaction with the antibody, a hypothesis consistent with the STD NMR data. The average root-mean-

square difference for superimposition of the 10 structures with the lowest NOE restraint energy was 0.46 Å for the backbone atoms (N, C_α, C, and O) of residues 51−57. The 10 structures superimposed with an rmsd of 1. 79 Å for backbone atoms considering the entire peptide (Table 3). There is more disorder in the terminal parts of the peptide, which are less well defined by the TRNOEs.

DISCUSSION

By interfering with cellular proteins such as β-TrCP, HIV-1 Vpu probably has a major effect on various functions and signaling pathways in HIV-1-infected cells. These consequences are still not fully understood. As β-TrCP controls essential cellular signaling pathways, by degrading β-catenin and IκBα substrates via the ubiquitin−proteasome system, it was recently shown that Vpu is a competitive inhibitor of β-TrCP that impairs the degradation of $SCF^{\beta-TrCP}$ substrates as long as Vpu has an intact D**pS**GNE**pS** phosphorylation motif and can bind to β-TrCP (*45*). The analysis of an X-ray crystal structures published recently (*46*, *47*) reveals the binding site specific for a phosphopeptide complex bound to a seven-bladed WD40 propeller domain in the SCF^{Cdc4} ubiquitin ligase (Figure 6c,d). A monoclonal antibody reacting specifically with Vpu phosphorylated at Ser52 and Ser56 is an essential tool in defining the interactions, distribution, and regulation of Vpu and its role in signal transduction.

Conformation of P-Vpu$^{41-62}$ Bound to mAb DE7. TRNOE NMR studies of the P-Vpu$^{41-62}$ peptide in the presence of mAb DE7 showed, for the bound conformation of the peptide, a propensity for turn formation in N-terminal residues 42−49, and a bend including the D**pS**^{52}GNE**pS**^{56} phosphorylation motif from residue Asp51 to Glu57 with the phosphate group pointing away (Figure 5). This bend would expose the side chains of residues 51−57 for specific interactions with the antibody combining site that is consistent with the STD NMR data, showing enhancements of the residues in the same region, between 60 and 100% (Figure 2).

The conformation of the mAb-bound P-Vpu$^{41-62}$ peptide (Figure 5), with formation of several bends in the I42−A49 and E50−E59 regions, is significantly represented in the free phosphorylated peptide (Figure 6a) (*12*) but is different from the structure of the segment found within the intact protein before phosphorylation (Figure 1c), two helical sections separated by a loop region (*48*). Structural studies of the Vpu protein have shown that the solution structure of the Vpu cytoplasmic domain, the free nonphosphorylated peptide, Vpu$^{32-81}$ (Figure 1c), adopts a well-defined helix (h2)−interconnection−helix (h3)−turn conformation, in which the four regions are bounded by residues 37−51, 52−56, 57−72, and 73−78 (*49*). The structural effect of phosphorylation at sites Ser52 and Ser56 of the P-Vpu$^{41-62}$ peptide, influenced the relatively flexible interconnection between α-helices h2 and h3 (Figure 6a) (*12*), has structural features different from those of the parent Vpu$^{41-62}$ peptide (Figure 1c) (*12*). α-Helix h2 was slightly shortened, and helix h3 disappears, replaced by a flexible extended "tail" for the C-terminal part. The structural rearrangements triggered by phosphorylation can account for the relative disorder of the helix.

In the presence of the antibody, the large bend (EDpSGNEpSE) connecting the helix of the hydrophilic cytoplasmic domain to the C-terminal coiled region interacts through hydrophobic and polar side chains. The bend (E50−E57) is probably inserted in the binding pocket of the mAb, as evidenced by the strong TRNOEs (<3.5 Å) observed between the backbone amides (Figure 4) and the shifts observed for the backbone amides in contact with the mAb epitope region (Figure 3).

The bend is similarly found in the mAb and also in the β-TrCP-bound P-Vpu$^{41-62}$ peptides (*16*), as shown in Figures 5b and 6b. To elucidate the basis of β-TrCP recognition, the structure of the P-Vpu$^{41-62}$ peptide bound to the F-box protein β-TrCP was previously determined by NMR and MD (*16*); residues 50−57 form a bend, while the phosphate groups point away. The β-turn motif also plays a central role in the crystal structure of the human β-TrCP1−Skp1 complex bound to a fragment β-catenin substrate peptide (*46*) (Figure 6c,d); of the β-catenin motif in the crystals, only an 11-residue segment (residues 30−40), centered on the doubly phosphorylated motif (D**pS**^{33}GXX**pS**^{37}), makes the largest number of β-TrCP contacts (Figure 6d). The phosphoserine, aspartic acid, and hydrophobic residues of the motif are recognized directly by contacts from β-TrCP1. Thus, the mAb-bound structure corresponds to the model's prediction of substrate recognition by the β-TrCP1 WD40 domain. Interaction of HIV-1 Vpu with the phosphorylation specific monoclonal antibody relies on the D**pS**GXX**pS** motif, similar to that found in the other substrates of β-TrCP (IκBα and β-catenin). The β-turn motif has also been observed in other cases, for many short, antigenic peptides bound to the antibodies (*32*, *43*, *44*, *50*), a conformation often observed in peptides containing Pro or Gly residues. The phosphorylated side chain is Ser, Thr, or His. This residue is often preceded or followed by a Gly; in most cases, the residue two positions further along the chain is a positively charged Lys or Arg. The Pro or the Gly binding pocket is able to accommodate other residues with the same propensity for forming β-turns. These sequences bear some resemblance to the phosphoryl-binding loop of various proteins (*51*).

Binding Region of P-Vpu$^{41-62}$ with mAb DE7. The STD NMR studies of the P-Vpu$^{41-62}$ peptide in the presence of mAb DE7 showed that the NH and aliphatic groups of Asp51, pSer52, Asn54, and Glu57 interact strongly with the corresponding amino acids inside the paratope (STD intensities between 60 and 100%). In addition, the NH and aliphatic groups of Leu45 and Ile46 residues are recognized (STD intensities, ranging from 70 to 90%), whereas the NH protons of Ser61 and Ala62 are less implicated (STD intensities between 20 and 30%). Except for Gly53, all the chain residues in the ED**pS**GNE**pS**E bend form a negatively charged surface that would provide a plausible binding region similar to the negative β-catenin substrate peptide in contact with the positive protein β-TrCP surface shown in Figure 6c. The position of Glu50, Asp51, pSer52, Glu55, pSer56, and Glu57 within a larger, extended epitope may be designed to present the phosphate group to antibodies. The phosphate group of pSer52 is able to make the largest number of contacts, in forming electrostatic interactions with some guanidinium group of Arg in mAb DE7, and hydrogen bonds with some hydroxyl groups of Tyr and Ser. Asp51, which is an invariant binding motif residue, is also able to make an extensive contact as its side chain allows a hydrogen bond

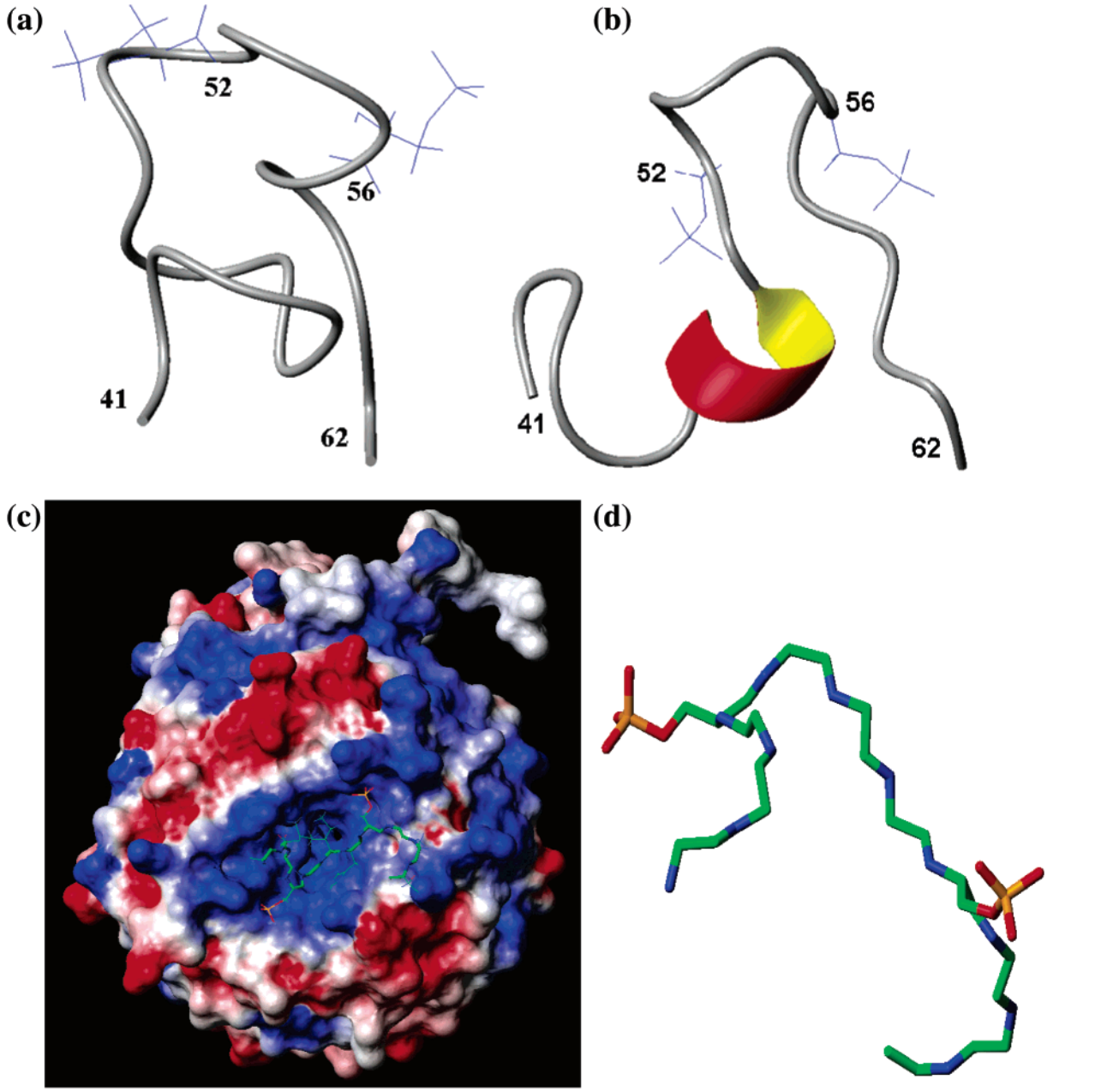

FIGURE 6: (a) Backbone (residues 41−62) of the minimum energy-minimized conformer of the free P-Vpu$^{41-62}$ peptide at pH 7.2. Domains of the secondary structural regions found in P-Vpu which contains phosphoserines pSer^{52} and pSer^{56} and in which helix 3 disappears. (b) NMR TRNOE-derived structure of the bound P-Vpu$^{41-62}$ peptide in the presence of the a GST−β-TrCP protein. (c) Surface representation of the top face of the β-TrCP WD40 domain with the bound D**pS**GXX**pS** motif from the crystal structure of the human β-TrCP−SkP1 complex bound to a β-catenin substrate peptide (*46*). The surface is colored according to the electrostatic potential (red for the negative region and blue for the positive surface). (d) Close-up view of the doubly phosphorylated D**pS**GXX**pS** motif bound, present in β-catenin, Vpu, and IκBα and recognized by the F-box protein β-TrCP (*46*).

with some Arg and Tyr in mAb DE7 to form. Gly53, also an invariant binding motif residue, is able to pack with the antibody receptor in an environment with little space for a non-glycine residue.

The NMR data described above show that the epitope comprises a surface extending over residues of the D**pS**^{52}GNE**pS**^{56} motif, with contributions being made by the main chain of hydrophobic residues Ile46 and Leu45. These observations are consistent with the sequence requirements playing a role in interaction with the β-TrCP protein (*16*), the bend D**pS**GXX**pS** motif of the bound P-Vpu$^{41-62}$ peptide associated with the hydrophobic cluster (Leu45 and Ile46). Leu45 and Ile46, whose hydrophobic nature is conserved in the peptide fragment, are able to make van der Waals contacts with a hydrophobic pocket that would be composed of the aliphatic portion of the Ala, Leu, and Val side chains in mAb DE7. The turn conformation is often important in allowing peptide side chains to be positioned correctly within the binding site and to make specific contacts with residues within the site. This is clearly important here as is shown by the epitope mapping data where Leu45 and Ile46 side chains and Arg48 and Glu57 side chains contact the site. Such information is valuable in understanding peptide-phosphorylated HIV-1-encoded virus protein U mimicry, where knowledge of the specific residues required for binding is necessary.

CONCLUSION

The refined conformation of the P-Vpu$^{41-62}$ peptide in the binding sites of its monoclonal antibody is necessary to understand the biological action of the overall Vpu protein phosphorylated at sites pSer52 and pSer56. A comparative analysis of the free and bound P-Vpu$^{41-62}$ structures underscores the importance of the β-strand as a structural consequence of the phosphorylation. The data presented here are important for refining the bound phosphorylated structures and provide valuable assistance in the interpretation of the NMR investigation of the complexes of these peptides linked to their binding proteins. Taken together, our data are consistent with the idea that the specific monoclonal antibody and β-TrCP interactions with the phosphorylated peptide are to a great extent analogous. The similarities observed in the P-Vpu$^{41-62}$ peptide (including the phosphorylation DpS^{52}-GNEpS^{56} motif) bound to its two receptors will facilitate understanding of the basic mechanisms involved in HIV−receptor interactions. The examination of P-Vpu conformations, while bound to β-TrCP, in conjunction with highly refined structures free in solution and in the antibody-bound states will provide a clearer picture of the biological actions of the release of the human immunodeficiency virus type 1 particle from infected cells and degradation of CD4 receptor molecules.

SUPPORTING INFORMATION AVAILABLE

Tables listing secondary structure analysis and dihedral angles for the bound structure with the lowest energy calculated for the P-Vpu$^{41-62}$ peptide in complex with mAb DE7 and some interresidue ^{1}H−^{1}H distances from unambiguous ROE and NOE volumes; figures showing a region of the TRNOESY spectrum of the P-Vpu$^{41-62}$ peptide in the presence of mAb DE7, for a peptide:antibody ratio of 10:1 in PBS solution and a NOESY spectrum of the P-Vpu$^{41-62}$ peptide without mAb DE7, recorded at 500 MHz and 280 K with the same mixing time of 200 ms; a figure showing TRNOE buildup rates of the P-Vpu$^{41-62}$ peptide in the presence of mAb DE7 plotted as volume TRNOE versus mixing time (milliseconds); a figure showing a region of the TRNOESY spectrum of the P-Vpu$^{41-62}$ peptide in the presence of mAb DE7, with a mixing time of 200 ms, and the same region of the TRROESY spectrum with a mixing time of 100 ms as ROE builds up twice as fast as NOE. This material is available free of charge via the Internet at http://pubs.acs.org.

REFERENCES

1. Marassi, F. M., Ma, C., Gratkowski, H., Straus, S. K., Strebel, K., Oblatt-Montal, M., Montal, M., and Opella, S. J. (1999) Correlation of the structural and functional domains in the membrane protein Vpu from HIV-1, *Proc. Natl. Acad. Sci. U.S.A. 96*, 14336−14341.
2. Strebel, K., Klimkait, T., Maldarelli, F., and Martin, M. A. (1989) Molecular and biochemical analyses of human immunodeficiency virus type 1 vpu protein, *J. Virol. 63*, 3784−3791.
3. Strebel, K., Klimkait, T., and Martin, M. A. (1988) A novel gene of HIV-1, Vpu, and its 16 kilodalton product, *Science 241*, 1221−1223.
4. Willey, R. L., Maldarelli, F., Martin, M. A., and Strebel, K. (1992) Human immunodeficiency virus type 1 Vpu protein induces rapid degradation of CD4, *J. Virol. 66*, 7193−7200.
5. Margottin, F., Bour, S., Durand, H., Selig, L., Benichou, S., Richard, V., Thomas, D., Strebel, K., and Benarous, R. (1998) A novel human WD protein, h-βTrCP, that interacts with HIV-1 Vpu connects CD4 to the ER degradation pathway through an F-box motif, *Mol. Cell 1*, 565−574.
6. Schubert, U., and Strebel, K. (1994) Differential activities of the human immunodeficiency virus type I-encoded Vpu protein are regulated by phosphorylation and occur in different cellular compartments, *J. Virol. 68*, 2260−2271.
7. Hart, M., Concordet, J.-P., Lassot, I., Albert, I., Del los Santos, R., Durand, H., Perret, C., Rubinfeld, B., Margottin, F., Benarous, R., and Polakis, P. (1999) The F-box protein β-TrCP associates with phosphorylated β-catenin and regulates its activity in the cell, *Curr. Biol. 9*, 207−210.
8. Winston, J. T., Strack, P., Beer-Romero, P., Chu, C. Y., Elledge, S. J., and Harper, J. W. (1999) The SCF β-TrCP-ubiquitin ligase complex associates specifically with phosphorylated destruction motifs in IκBα and β-catenin and stimulates IκBα ubiquitination in vitro, *Genes Dev. 13*, 270−283.
9. Yaron, A., Hatzubai, A., Davis, M., Lavon, I., Amit, S., Manning, A. M., Andersen, J. S., Mann, M., Mercurio, F., and Ben-Neriah, Y. (1998) Identification of the receptor component of the IκBα-ubiquitin ligase, *Nature 396*, 590−594.
10. Kroll, M., Margottin, F., Kohl, A., Renard, P., Durand, H., Concrodet, J.-P., Bachelerie, F., Arenzana-Seisdedos, F., and Benarous, R. (1999) Inducible degradation of IκBα by the proteasome requires interaction with the F-box protein h-βTrCP, *J. Biol. Chem. 274*, 7941−7945.
11. Lassot, I., Ségéral, E., Berlioz-Torrent, C., Durand, H., Groussin, L., Hai, T., Benarous, R., and Margottin-Goguet, F. (2001) ATF4 Degradation Relies on a Phosphorylation-Dependent Interaction with the SCFβ-TrCP Ubiquitin Ligase, *Mol. Cell. Biol. 21*, 1−11.
12. Coadou, G., Evrard-Todeschi, N., Gharbi-Benarous, J., Benarous, R., and Girault, J.-P. (2002) HIV-1 encoded virus protein U (Vpu). Solution structure of the 41−62 hydrophilic region containing the phosphorylated sites Ser^{52} and Ser^{56}, *Int. J. Biol. Mol. 30*, 23−40.
13. Taub, R., Gould, R. J., Garsky, V. M., Ciccarone, T. M., Hoxie, J., Friedman, P. A., and Shattil, S. J. (1989) A monoclonal antibody against the platelet fibronogen receptor contains a sequence that mimics a receptor recognition domain in fibrinogen, *J. Biol. Chem. 264*, 259−265.
14. Taub, R., and Greene, M. I. (1992) Functional validation of ligand mimicry by anti-receptor antibodies: structural and therapeutic implications, *Biochemistry 31*, 7431−7435.
15. Calvete, J. J., Schafer, W., Mann, K., Henschen, A., and Gonzalez-Rodriguez, J. (1992) Localization of the cross-linking sites of RGD and KQAGDV peptides to the isolated fibrinogen receptor, the human platelet integrin glycoprotein IIb/IIIa. Influence of peptide length, *Eur. J. Biochem. 206*, 759−765.
16. Coadou, G., Gharbi-Benarous, J., Megy, S., Bertho, G., Evrard-Todeschi, N., Segeral, E., Benarous, R., and Girault, J. P. (2003) NMR Studies of the Phosphorylation Motif of the HIV-1 Protein Vpu Bound to the F-Box Protein β-TrCP, *Biochemistry 42*, 14741−14751.
17. Ni, F. (1994) Recent Developments in Transferred NOE Methods, *Prog. Nucl. Magn. Reson. Spectrosc. 26*, 517−606.
18. Klein, J., Meinecke, R., Mayer, M., and Meyer, B. (1999) Detecting binding affinity to immobilized receptor proteins in compound libraries by HR-MAS STD NMR, *J. Am. Chem. Soc. 121*, 5336−5337.
19. Mayer, M., and Meyer, B. (1999) Characterization of ligand binding by saturation transfer difference NMR spectroscopy, *Angew. Chem., Int. Ed. Engl. 38*, 1784−1788.
20. Mayer, M., and Meyer, B. (2001) Group epitope mapping by saturation transfer difference NMR to identify segments of a ligand in direct contact with a protein receptor, *J. Am. Chem. Soc. 123*, 6108−6117.
21. Otting, G. (1993) Experimental NMR techniques for studies of protein−ligand interactions, *Curr. Open. Struct. Biol. 3*, 760−768.
22. Verdier, L., Gharbi-Benarous, J., Bertho, G., Mauvais, P., and Girault, J. P. (2002) Antibiotic Resistance Peptides; Interaction of Peptides Conferring Macrolides and Ketolide Resistance with *Staphylococcus aureus* Ribosomes. Conformation of Bound Peptides As Determined by Transferred NOE Experiments, *Biochemistry 41*, 4218−4229.
23. Cung, M. T., Demange, P., Marraud, M., Tsikaris, V., Sakarellos, C., Papadouli, I., Kokla, A., and Tzartos, S. J. (1991) Two-dimensional ^{1}H-NMR study of antigene-antibody interactions:

Binding of synthetic decapeptides to an anti-acetylcholine receptor monoclonal antibody, *Biopolymers 31*, 769−776.
24. Cung, M. T., Marraud, M., Tsikaris, V., Sakarellos, C., Papadouli, I., and Tzartos, S. J. (1992) Etude par RMN-2D des interactions antigène-anticorps: reconnaissance des analogues décapeptidiques du fragment α67−76 du récepteur RACh par les anticorps anti-RACh, *J. Chim. Phys. 89*, 167−173.
25. Petit, M. C., Orlewski, P., Tsikaris, V., Sakarellos-Daitsiotis, M., Sakarellos, C., Tzinia, A., Konidou, G., Soteriadou, K. P., Marraud, M., and Cung, M. T. (1998) Solution structures of the fibronectin-like *Leishmania* gp63 SRYD-containing sequence in the free and antibody-bound states. Transferred NOE and molecular dynamics studies, *Eur. J. Biochem. 253*, 184−193.
26. States, D. J., Haberkorn, R. A., and Ruben, D. J. (1982) *J. Magn. Reson. 48*, 286−292.
27. Piotto, M., Saudek, V., and Sklenar, V. (1992) Gradient-tailored exitation for single-quantum NMR spectroscopy of aqueous solutions, *J. Biol. NMR 2*, 661−665.
28. Bax, A., and Davis, D. G. (1985) MLEV-17-based two-dimensional homonuclear magnetization transfer spectroscopy, *J. Magn. Reson. 65*, 355−360.
29. Meyer, B., and Peters, T. (2003) NMR spectroscopy techniques for screening and identifying ligand binding to protein receptors, *Angew. Chem., Int. Ed. Engl. 42*, 864−890.
30. Clore, G. M., and Gronenborn, A. M. (1983) Theory of the Time Dependent Transferred Nuclear Overhauser Effect: Applications to Structural Analysis of Ligand-Protein Complexes in Solution, *J. Magn. Reson. 53*, 423−442.
31. Kumar, A., Wagner, G., Ernst, R. R., and Wüthrich, K. (1981) Buildup rates of the NOE measured by 2D Proton Magnetic Resonance Spectroscopy: Implication for studies of protein conformation, *J. Am. Chem. Soc. 103*, 3654−3658.
32. Johnson, M. A., Jaseja, M., Zou, W., Jennings, H. J., Copié, V., Pinto, B. M., and Pincus, S. H. (2003) NMR Studies of Carbohydrates and Carbohydrate-mimetic Peptides Recognized by an Anti-Group B *Streptococcus* Antibody, *J. Biol. Chem. 278*, 24740−24752.
33. Vincent, S. J., Zwahlen, C., Post, C. B., Burgner, J. W., and Bodenhausen, G. (1997) The conformation of NAD^+ bound to lactate dehydrogenase determined by nuclear magnetic resonance with suppression of spin diffusion, *Proc. Natl. Acad. Sci. U.S.A. 94*, 4383−4388.
34. Zwahlen, C., Vincent, S. J., Ziegler, A., and Bodenhausen, G. (1994) Characteristic patterns of metabolites from selective two-dimensional proton NMR, *J. Magn. Reson., Ser. B 103*, 299−302.
35. Brünger, A. T., Adams, P. D., Clore, G. M., DeLano, W. L., Gros, P., Grosse-Kunstleve, R. W., Jiang, J. S., Kuszewski, J., Nilges, M., Pannu, N. S., Read, R. J., Rice, L. M., Smonson, T., and Warren, G. L. (1998) Crystallography & NMR system: a new software suite for macromolecular structure determination, *Acta Crystallogr. D54*, 905−921.
36. Linge, J. P., Habeck, M., Rieping, W., and Nilges, M. (2003) ARIA: automated assignment and NMR structure calculation, *Bioinformatics 19*, 315−316.
37. Brooks, B. R., Bruccoleri, R. E., Olafson, B. D., States, D. J., Swaminathan, S., and Karplus, M. (1983) CHARMM: A Program for Macromolecular Energy, Minimization, and Dynamics Calculations, *J. Comput. Chem. 4*, 187−217.
38. Schibli, D. J., Monelero, R. C., and Vogel, H. J. (2001) The Membrane-Proximal Tryptophan-Rich Region of the HIV Glycoprotein, gp41, Forms a Well-Defined Helix in Dodecylphosphocholine Micelles, *Biochemistry 40*, 9570−9578.
39. Koradi, R., Billeter, M., and Wüthrich, K. (1996) MOLMOL: a program for display and analysis of macromolecular structures, *J. Mol. Graphics 14*, 51−55.
40. Wüthrich, K. (1986) *NMR of Proteins and Nucleic Acids*, John Wiley & Sons, New York.
41. Kooistra, O., Herfurth, L., Luneberg, E., Frosch, M., Peters, T., and Zahringer, U. (2002) Epitope mapping of the O-chain polysaccharide of *Legionella pneumophila* serogroup 1 lipopolysaccharide by saturation-transfer-difference NMR spectroscopy, *Eur. J. Biochem. 269*, 573−582.
42. Clore, G. M., and Gronenborn, A. M. (1982) Theory and Applications of the Transferred Nuclear Overhauser Effect to the Study of the Conformations of Small Ligands Bound to Proteins, *J. Magn. Reson. 48*, 402−417.
43. Phan-Chan-Du, A., Hemmerlin, C., Krikorian, D., Sakarellos-Daitsiotis, M., Tsikaris, V., Sakarellos, C., Marinou, M., Thureau, A., Cung, M. T., and Tzartos, S. (2003) Solution Conformation of the Antibody-Bound Tyrosine Phosphorylation Site of the Nicotinic Acetylcholine Receptor β-Subunit in Its Phosphorylated and Nonphosphorylated States, *Biochemistry 42*, 7371−7380.
44. Phan-Chan-Du, A., Petit, M. C., Guichard, G., Briand, J. P., Muller, S., and Cung, M. T. (2001) Structure of antibody-Bound Peptides and Retro-Inverso Analogues. A Transferred Nuclear Overhauser Effect Spectroscopy and Molecular Dynamics Approach, *Biochemistry 40*, 5720−5727.
45. Besnard-Guerin, C., Belaidouni, N., Lassot, I., Segeral, E., Jobart, A., Marchal, C., and Benarous, R. (2004) HIV-1 Vpu sequesters β-transducin repeat-containing protein (betaTrCP) in the cytoplasm and provokes the accumulation of β-catenin and other SCFbetaTrCP substrates, *J. Biol. Chem. 279*, 788−795.
46. Wu, G., Xu, G., Schulman, B. A., Jeffrey, P. D., Harper, J. W., and Pavletich, N. P. (2003) Structure of a β-TrCP1−Skp1-β-catenin complex: destruction motif binding and lysine specificity of the SCF(β-TrCP1) ubiquitin ligase, *Mol. Cell 11*, 1445−1456.
47. Orlicky, S., Tang, X., Willems, A., Tyers, M., and Sicheri, F. (2003) Structural Basis for Phosphodependent Substrate Selection and Orientation by the SCF^{Cdc4} ubiquitin ligase, *Cell 112*, 243−256.
48. Willbold, D., Hoffmann, S., and Rosch, P. (1997) Secondary structure and tertiary fold of the human immunodeficiency virus protein U (Vpu) cytoplasmic domain in solution, *Eur. J. Biochem. 245*, 581−588.
49. Federau, T., Schubert, U., Flossdorf, J., Henklein, P., Schomburg, D., and Wray, V. (1996) Solution structure of the cytoplasmic domain of human immunodeficiency virus type 1 encoded virus protein U (Vpu), *Int. J. Pept. Protein Res. 47*, 297−310.
50. Campbell, P. A., Wong, W. Y., Irvin, R. T., and Sykes, B. D. (2000) Interaction of a Bacterially Expressed Peptide from the Receptor Binding Domain of *Pseudomonas aeruginosa* Pili Strain PAK with a Cross-Reactive Antibody: Conformation of the bound peptide, *Biochemistry 39*, 14847−14864.
51. Williams, R. E. (1976) phosphorylated sites in substrates of intracellular protein kinases. A common feature in amino acid sequences, *Science 192*, 473−474.

BI0492861